Update on the Heavy Photon Search Experiment

C. Bravo, P. Butti, C. Field, S. Gaiser, M. Graham, R. Herbst,
J. Jaros, T. Nelson[a,b], E. Peets, B. Reese, P. Schuster, N. Toro

SLAC National Accelerator Laboratory, Menlo Park, CA 94025

L. Tompkins, R. O'Dwyer

Stanford University, Stanford, CA 94305

V. Fadeyev, R. Johnson, A. Spellman

University of California, Santa Cruz, CA 95064

P. Achenbach, N. Baltzell, S. Boyarinov, T. Cao, C. Cuevas, A. Deur,
R. De Vita, H. Egiyan, V. Kubarovsky, R. Paremuzyan, B. Raydo,
S. Stepanyan[a], M. Ungaro, H. Szumila-Vance, B. Wojtsekhowski

Thomas Jefferson National Accelerator Facility, Newport News, Virginia 23606

R. Essig

Stony Brook University, Stony Brook, NY 11794-3800

M. Holtrop[a], L. Wolf

University of New Hampshire, Department of Physics, Durham, NH 03824

G. Charles, R. Dupre, D. Marchand, C. Munoz-Camacho, S. Niccolai

Institut de Physique Nucleaire d'Orsay, IN2P3, BP 1, 91406 Orsay, France

N. Dashyan, N. Gevorgyan, H. Voskanyan

Yerevan Physics Institute, 375036 Yerevan, Armenia

M. Battaglieri, A. Celentano, L. Marsicano

Istituto Nazionale di Fisica Nucleare, Sezione di Genova, Italy

S. Bueltmann

Old Dominion University, Norfolk, Virginia 23529

M. Bondí, M. De Napoli, N. Randazzo

Istituto Nazionale di Fisica Nucleare, Sezione di Catania, Italy

[a]Co-spokesperson
[b]Contact person

M. Carpinelli

Università di Milano Bicocca, Dipartimento di Fisica e INFN, 20126 Milano MI, Italy

D. D'Urso, V. Sipala

Università di Sassari and Istituto Nazionale di Fisica Nucleare, 07100 Sassari, Italy

G. Simi

Dipartimento di Fisica e Astronomia, Università di Padova and Istituto Nazionale di Fisica Nucleare, Sezione di Padova, Padova, Italy

A. D'Angelo

Dipartimento di Fisica dell'Università Tor Vergata, Roma and Istituto Nazionale di Fisica Nucleare, Sezione di Roma-TorVergata, Italy

A. Filippi

Istituto Nazionale di Fisica Nucleare, Sezione di Torino, Torino, Italy

B. McKinnon, D. Sokhan

University of Glasgow, Glasgow G12 8QQ, United Kingdom
(Dated: May 8, 2024)

EXECUTIVE SUMMARY

The Heavy Photon Search (HPS) experiment in Hall-B at Jefferson Lab searches for heavy or dark photons that mix with ordinary photons through kinetic mixing, which induces their weak coupling to electrons, ϵe, and therefore can be produced in electron bremsstrahlung and subsequently decay into e^+e^-. The experiment exploits resonance and displaced vertex signatures to search for these hypothetical particles over a wide range of couplings, $\epsilon^2 > 10^{-10}$, and masses, $20\,\mathrm{MeV/c^2} < m_{A'} < 220\,\mathrm{MeV/c^2}$, using a compact, large-acceptance forward spectrometer consisting of a tungsten foil target, a silicon micro-strip vertex tracker (SVT), a $PbWO_4$ electromagnetic calorimeter (ECal), and a scintillation hodoscope (SH). Since the last jeopardy update to PAC48 in 2020, HPS has used 30 out of the remaining 135 PAC days for the second physics run. The HPS collaboration continues the analysis and calibration of data on hand. We published the results of A' searches using the resonance and displaced vertex signatures from engineering run data sets. We are also actively performing the detector maintenance and repair work to prepare for further operations to complete HPS data-taking, while we continue to improve the calibration and analysis of the 2019 and 2021 data sets. Included in this update are summaries of recently published results, the status of calibration and reconstruction of the newest datasets, new improvements to our search methodologies, and the latest developments in expanding the search for heavy photons to include additional signatures. With this update, we request approval of the remaining 105 PAC days of beamtime, about 60% of which we plan to run in late 2025 or 2026 with two-pass ($\simeq 4\,\mathrm{GeV}$) and the rest with one-pass ($\simeq 2\,\mathrm{GeV}$) electron beams in the future.

1. MOTIVATION AND HISTORY

Establishing the nature of dark matter is one of the major open challenges of modern physics. The LHC, as well as direct and indirect detection experiments, have significantly constrained one of the best-motivated weak-scale dark matter models with a class of particle candidates known as weakly interacting massive particles (WIMPs). In contrast, similarly motivated scenarios involving light hidden sector dark matter with mediators in the MeV-GeV range are relatively unexplored and remain one of the simplest mechanisms by which dark matter can interact with ordinary matter, which allows the dark matter to be produced from Standard Model particles in the hot thermal plasma present in the early Universe [1]. Models with a broken hidden-sector $U(1)$ gauge symmetry, giving rise to a "dark" or "hidden sector" photon, are particularly attractive and can be tested experimentally. Such hidden-sector gauge symmetries are common in theories beyond the Standard Model, and have long been recognized as giving rise to a simple and appealing portal from the Standard Model sector to this hidden sector [2]. Dark photons also provide a simple mechanism by which dark matter particles can interact with themselves through non-gravitational forces; such "self-interactions" provide an explanation for the observed distribution of dark matter on "small" (∼kiloparsec-size) scales in galaxies and galaxy clusters in the Universe. These puzzles are commonly and collectively referred to as the "small-scale problems of cold dark matter", where cold dark matter refers to non-relativistic, collisionless dark matter particles, i.e., particles that do not self-interact (such as WIMPs).

If they exist, heavy photons undergo kinetic mixing with ordinary photons, which induces their weak coupling to charged particles, ϵq, where q is the particle's charge and $\epsilon \leq 10^{-2}$, giving rise to a multitude of signatures at colliders, fixed-target experiments, direct-detection experiments, in astrophysical systems, and in cosmology. In particular, since they couple to electrons, heavy photons are radiated in electron scattering and can subsequently decay into an e^+e^-. If ϵ is large enough, $\epsilon^2 \gtrsim 10^{-7}$, they would appear as a narrow mass peak in the e^+e^- invariant mass distribution, which can be observed as a resonance atop the continuum of QED trident background. For suitably small couplings, $\epsilon^2 < 10^{-8}$, heavy photons travel detectable distances before decaying, providing the second signature of a displaced vertex. The Heavy Photon Search (HPS) experiment in Hall-B at JLab exploits both these signatures to search for heavy photons over a wide range of couplings, $\epsilon^2 > 10^{-10}$, and masses, $20\,\mathrm{MeV/c^2} < m_{A'} < 220\,\mathrm{MeV/c^2}$, using a compact, large-acceptance forward spectrometer consisting of a silicon microstrip vertex tracker (SVT), a $PbWO_4$ electromagnetic calorimeter (ECal), and a scintillation hodoscope (SH).

The first HPS proposal was presented to PAC 37 in 2011 [3], which recommended conditional approval C2 for 180 PAC days contingent upon a successful Test Run. The Test Run experiment was funded and built in time for commissioning early in 2012, where it ran parasitically on a photon beam in Hall B. Early results from the test run were published [4] and presented to PAC 39 in 2012 [5], which boosted HPS approval to C1 with an "A" rating. HPS proceeded with the design of the full experiment, proposed to DOE HEP in the summer of 2013 and funded that fall subsequent to a review attended by JLab management. In Spring 2014, HPS requested formal approval from JLab, which granted 25 PAC days for an engineering run and requested performance demonstrations before granting additional time. Later that spring, PAC 41 selected HPS for "High Impact Status". HPS completed two engineering runs in 2015 and 2016 with 1.056 GeV and 2.3 GeV beams, respectively. The small data samples from the engineering runs led to the first physics results from HPS, including seven PhD dissertations and the performance demonstrations JLab had requested [6, 7]. JLab accordingly granted HPS unconditional approval. Data from the engineering runs have led to an improved understanding of backgrounds and better calculations of physics processes, motivated important upgrades of the SVT and trigger system, and continue to be used to develop new reconstruction techniques and search methodologies. Upgrades to the apparatus were approved by DOE OHEP and completed in advance of a pair of physics runs in late FY19 and FY21. The 2019(2021) run at 4.56 GeV(3.74 GeV) collected roughly 53%(84%) of the expected datasets. These datasets are sufficient to explore important and uncharted regions in mass and coupling, discovering dark photons or excluding them, with the first results expected in the coming year. After maintenance and repair work, funded and currently underway, the detector will be ready for further operations to complete HPS data-taking.

The landscape of heavy photon searches has evolved since the first HPS proposal. While significant regions of parameter space have been ruled out, new target regions, motivated by hidden sector scenarios of sub-GeV dark matter, have emerged [1]. The past few years have also seen tremendous progress in understanding and elucidating the interactions that sub-GeV dark matter might have with the Standard Model. It was realized that interactions mediated by dark photons with masses in the MeV to GeV scale are among the least constrained possibilities and also give rise to several mechanisms that allow sub-GeV dark matter to be produced in the early Universe with a relic abundance that is consistent with the observed dark matter abundance. The parameter space that HPS will probe using displaced searches with 2 GeV to 5 GeV electron beams lies in the most highly motivated region for dark photon mediated dark matter, as well as probing newer models that also include rich dynamics in a light dark sector, such as SIMPs and inelastic dark matter [8][9]. Improvements being developed for the resonance search also hold promise in making HPS newly competitive at larger couplings. Meanwhile, there is stiff worldwide competition for this physics from experiments currently taking data or coming online in the next few years.

In this update, we present the operational history and status of the HPS experiment, the status of reconstruction and analysis of HPS datasets, and the status of recent advances in search methodologies and plans for expanding HPS searches to a broader palette of heavy photon physics. The run plan and expected reach from future operations is also presented, where HPS has used 75 of the approved 180 PAC days to date, and we request re-approval of the remaining 105 PAC days, including 60 PAC days requested and planned in FY25 or early FY26 with two-pass beam, as discussed in Section 4.

2. HPS APPARATUS, OPERATIONS, AND DATASETS

2.1. The HPS Detector

The sensitivity of the HPS experiment depends on two signatures of a heavy photon; reconstruction of an e^+e^- invariant mass peak and reconstruction of the e^+e^- production vertex. Meanwhile, the experiment must contend with copious production of QED trident and converted wide-angle, hard-bremsstrahlung (WAB) events with the same final state at rates that are higher by many orders of magnitude – roughly a factor of $1/\epsilon^2$. Since heavy photon production goes as $1/m_{A'}^2$, sensitivity is best in the regime $E_{\text{beam}} \gg m'_A$, where the A' is highly boosted and the resulting e^+e^- are nearly collinear with the beam. Therefore, a detector with excellent forward acceptance immediately downstream of the target is required to identify the e^+e^- pairs and cleanly reconstruct secondary vertices as close to the target and through-going scattered beam as possible.

HPS realizes this concept with a magnetic spectrometer, using a multi-layer Silicon Vertex Tracker (SVT) situated within a large dipole magnet to measure the momenta and trajectories of the e^+e^- pair, as shown in Figure 1. The field of the dipole is vertical, dispersing most of the beam electrons that have radiated in the target, as well as other electromagnetic backgrounds, into the horizontal plane containing the beam. As a result, the detector is split into two segments, one above and one below the beam plane, which are positioned as close to it as possible – 500 microns in the SVT layer closest to the target – to maximize acceptance. The extent of the forward acceptance

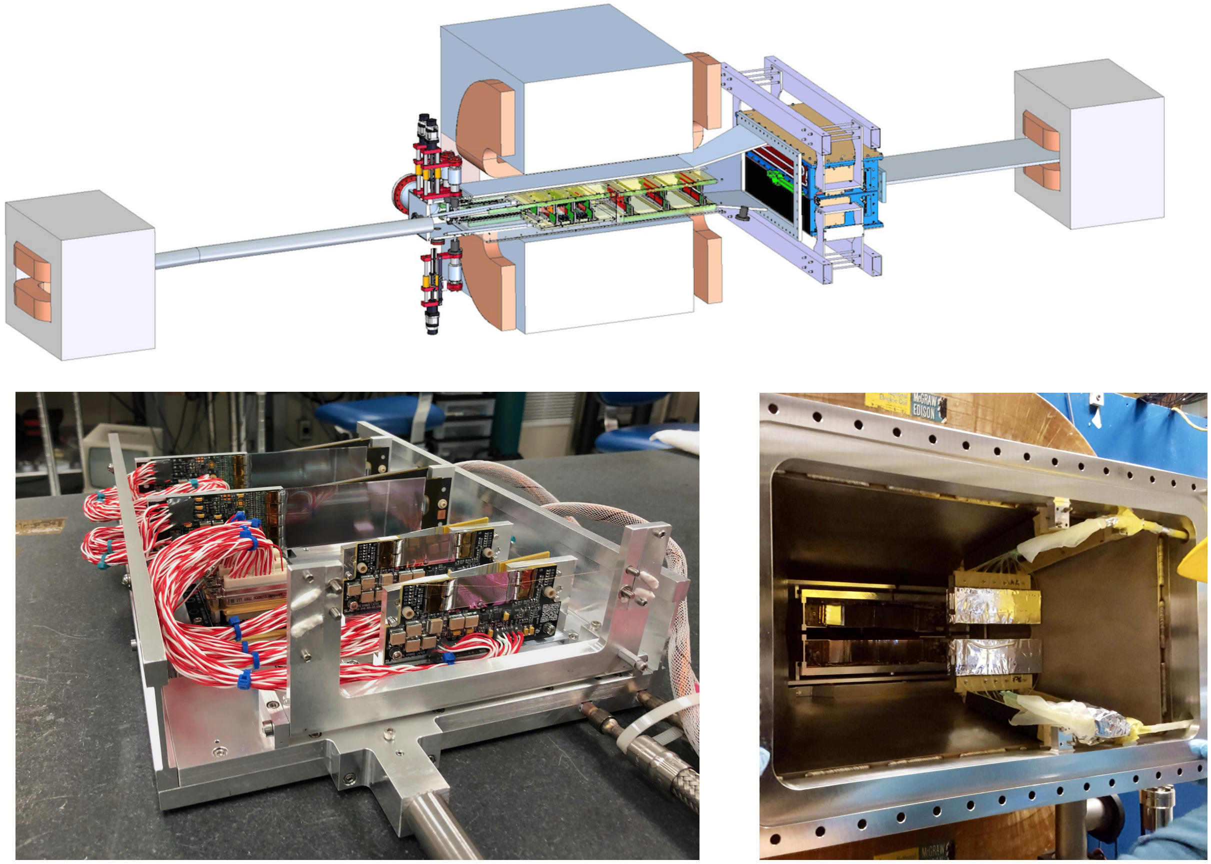

FIG. 1. Top: The engineering design of the baseline HPS detector showing the SVT inside a vacuum chamber in the spectrometer magnet and the ECal downstream. Bottom Left: One half of the front section of the SVT after upgrades to add a seventh tracking station closer to the target. Bottom Right: The back of the SVT showing the positron hodoscope upgrade inside the SVT vacuum chamber.

is limited by the background rate of single beam electrons that scatter in the target, which cannot mimic the signal but create radiation damage and extreme occupancies ($\approx 5-10\,\mathrm{MHz/mm^2}$) at the edge of the first layer of the SVT. The trigger is provided by the combination of a lead-tungstate electromagnetic calorimeter (ECal) and a scintillating hodoscope (SH), which identifies signal-like e^+e^- events for readout.

The detector installed in 2015 and operated for the engineering runs is shown in Figure 1, where the SVT consisted of six double-layers of single-sided silicon microstrips with a small stereo angle in each station to provide 3-D tracking with minimal multiple scattering. Readout of multiple samples per trigger allows reconstruction of pulse height with $S/N \gtrapprox 20$ and time resolution of $\approx 2\,\mathrm{ns}$. Meanwhile, the trigger was provided only by the ECal on pairs of high energy clusters in opposite quadrants within $4\,\mathrm{ns}$ windows. Upon initial analysis of 2015 data, it was recognized that a more aggressive approach to both tracking and triggering was possible and necessary to achieve the goals of the experiment. Success operating the SVT so close to the beam inspired an upgrade to add a layer of custom, slim-edge sensors a factor of two closer to the target to provide a commensurate improvement in vertex resolution, and to move other layers closer to improve acceptance for long-lived particles. Meanwhile, the rates of positrons measured by the engineering runs showed the feasibility of adding a small hodoscope to create a positron-only trigger. This trigger captures events where the corresponding electron in the final state escapes through the hole in the ECal near the through-going beam, which is necessitated by the overwhelming rate of scattered beam electrons in this region. The upgraded elements of the SVT and the SH are shown in Figure 1 and were installed in advance of HPS physics runs in 2019 and 2021.

2.2. HPS Engineering Runs and Data

The HPS apparatus was first operated during a pair of short engineering runs in 2015 and 2016. In May 2015, HPS commissioned the beamline and detectors using a 1.056 GeV beam at 50 nA, establishing the small beamspot size, excellent stability, and minimal halo required to move the SVT into position to take physics data, with the edge of the first layer 500 μm from the center of the beam. With commissioning complete, HPS accumulated 10 mC of data on a 4 μm target, corresponding to 1.17 pb^{-1} of physics data. The 2016 Engineering Run took place the following spring at 2.3 GeV with 200 nA beam and an 8 μm target. Re-commissioning was completed quickly, allowing the collection of 92.5 mC on target, corresponding to 10.6 pb^{-1} of physics data. Beamline performance, ECal energy and time resolution, trigger rate and acceptance, track finding efficiency, momentum and vertex resolution all met performance requirements and made the case for full HPS approval, which JLab granted in the spring of 2016.

Data from the 2015 Engineering Run provided the first opportunity to develop the complete physics analyses for the prompt resonance and displaced vertex searches, culminating in a pair of Ph.D. dissertations and the first physics publication [10]. These early analyses illuminated some previously unseen challenges in the form of unanticipated backgrounds and acceptance effects and identified where key improvements to the HPS detector could overcome them. This motivated upgrades to the SVT and the addition of the Scintillator Hodoscope, as described in Section 2.1, to improve the vertex resolution of the SVT and the signal acceptance of the SVT and trigger systems. These first searches also showed where analysis improvements would be important to achieving the full potential of the experiment, which will be discussed further in Section 3.

2.3. HPS Physics Runs and Data

Plans for the first physics run of the upgraded HPS apparatus called for 31 PAC days during the period June 17 – August 18, 2019, at a 4.5 GeV beam energy with a current of 300 nA on an 8 μm tungsten target. With one week for setup, this would yield 725 mC of charge on target, for an integrated luminosity of 229 pb^{-1}. Infrastructure and beam delivery issues delayed first physics data until July 26 and damaged SVT readout electronics and sensors, rendering some modules inoperable. JLab management extended the run by three weeks, to September 9^{th}, to partially offset the lost time, and HPS ultimately collected 122 pb^{-1} of data, 53% of the expected total. While loss of data from some SVT modules creates challenges for calibration and analysis, the performance of the upgrades was largely as expected.

Soon after the 2019 run, HPS was scheduled to operate again for 60 days during the summer of 2021 at a beam energy of 3.74 GeV. Assuming typical 50% uptime, the resulting dataset would correspond to roughly four PAC weeks and a total luminosity of 200 pb^{-1}. Prior to operation, HPS performed maintenance on the detector, including repairing damage to the SVT sustained during operations in 2019. In particular, the front-end boards – damaged by radiation – were completely replaced with a more robust design, and damaged modules in the first two layers were replaced by new modules using an improved sensor design. Together with improvements to beamline diagnostics and tuning procedures, these changes were intended to protect against a recurrence of the issues experienced in 2019.

Although the pandemic created challenges in completing these projects – work restrictions, travel restrictions, and supply chain issues – repairs to the detector were completed in time for the beginning of operations in September 2021. Similarly, the operation of the detector, much of which was done remotely, went relatively smoothly amidst the obstacles created by pandemic restrictions. Efforts to harden and protect the detector with improved procedures successfully avoided the kinds of damage observed in 2019. With much better beam conditions, HPS collected $168\,\mathrm{pb}^{-1}$ over 29 PAC days between September 9 and November 5, which was 84% of the total expected. With fewer data quality issues than in 2019, work to calibrate and optimize the reconstruction of 2021 data has proceeded more rapidly, and with similar beam energies, and therefore reach in the same region of parameter space, we anticipate analyzing 2019 and 2021 data in tandem to produce combined results. Meanwhile, before further operations, maintenance and repair of the SVT will be performed, including replacement of the modules in the first layers, replacement of some older modules with a significant fraction of dead channels, and rebuilding a pool of spares for the SVT DAQ. In addition, minor work on the ECal and updates to the trigger and back-end DAQ will also be completed.

3. ANALYSIS AND RESULTS

HPS can search for dark photons via multiple signatures, shown in Table I along with the attributes of the three major sources of background; radiative tridents, Bethe-Heitler tridents, and converted wide-angle hard bremsstrlung events.

	Signal				**Background**		
Signature	Minimal A' $\epsilon^2 \gtrsim 10^{-7}$	Minimal A' $\epsilon^2 \lesssim 10^{-8}$	SIMPs	iDM	radiative	Bethe-Heitler	Converted WAB
$x = \frac{\lvert p_{e^+}+p_{e^-}\rvert}{E_{\mathrm{beam}}}$	high	high	low	low	high	low	medium
resonance	**yes**	**yes**	**yes**	no	no	no	no
prompt/displaced	prompt	**displaced**	**displaced**	**displaced**	prompt	prompt	prompt

TABLE I. The key signatures of different A' models in HPS, and the corresponding attributes of the three major classes of QED backgrounds. These features are the foundation of the sensitivity to dark photons with HPS.

In the minimal A' model, the only assumption is that A' decays to dark sector particles are kinematically disallowed so that on-shell A' must decay back to Standard Model particles. With no other particles in the final state, the A' carries away most of the beam momentum so that $x = \mathrm{P_{Sum}}/E_{\mathrm{beam}}$ is peaked near unity, where $\mathrm{P_{Sum}} = |p_{e^+} + p_{e^-}|$. While this is kinematically identical to radiative QED tridents, the dominant QED background from Bethe-Heitler tridents peaks at low x. HPS searches for these minimal dark photons both at larger couplings, where A' are produced abundantly but decay promptly, so can only be distinguished by observing the e^+e^- resonance atop much larger QED backgrounds, and at smaller couplings, where few A' are produced but their decays can also be distinguished by their long lifetime. Results from these searches using data from the engineering runs are published in [10] and [11] and will be discussed in Sections 3.1 and 3.2.

In models with other light degrees of freedom in the dark sector, such as SIMPs and iDM, dark particles in the final state carry away energy so the signal tends to have $x < 1$. Meanwhile, for SIMPs, as in the minimal A' case, the e^+e^- pair in the final state comes from an on-shell A', while for iDM, the A' is virtual so that there is no resonant structure. However, both SIMPs and iDM are characterized by long-lived decays, which is a powerful tool in rejecting QED backgrounds. Searches for these signatures will be discussed in Section 3.3.

These key attributes of signal events – the e^+e^- $\mathrm{P_{Sum}}$, an e^+e^- resonance, and an e^+e^- displaced vertex – give rise to three foundational performance metrics for all HPS analyses and provide a snapshot of progress towards the final calibrations needed to produce results. The first of these, the momentum sum of the e^+e^- pair, is the key to understanding the signal acceptance and background rates for any of the A' searches. This distribution is shown in Figure 2 for the 2016, 2019, and 2021 datasets, where the prominence of the radiative peak at high $\mathrm{P_{Sum}} = |p_{e^+} + p_{e^-}|$ is critical for the minimal A' searches and the acceptance at low $\mathrm{P_{Sum}}$ is required for SIMPs and iDM. Up to differences in event selection, the acceptance and resolution at both low and high $\mathrm{P_{Sum}}$ using current calibrations for 2019 and 2021 data are similar to those for the final 2016 calibrations from [11]. The second attribute is the e^+e^- invariant mass, where the resolution is dominated by

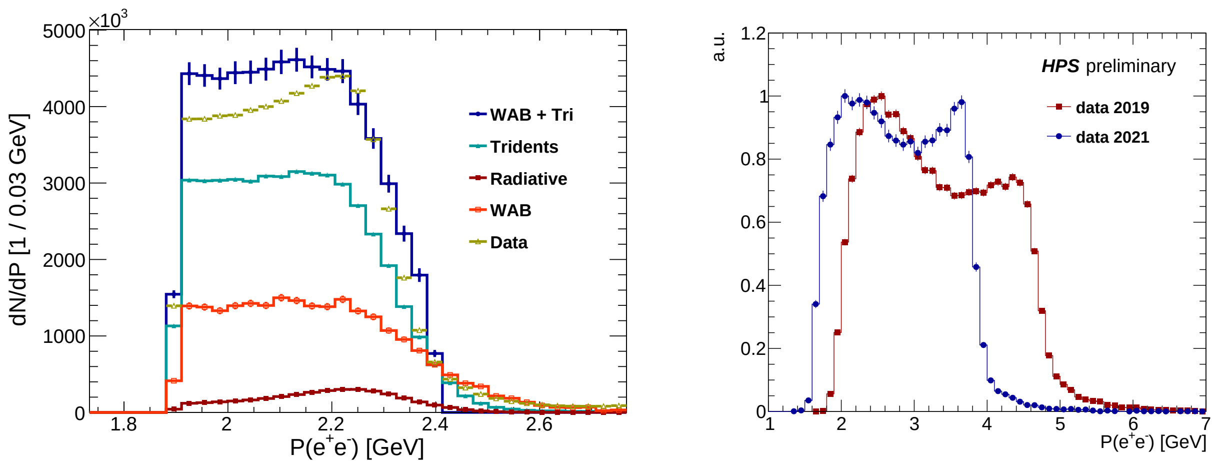

FIG. 2. Left: The distribution of $\mathrm{P_{Sum}}$ in 2016 data [11] showing the high $\mathrm{P_{Sum}}$ region. Right: The $\mathrm{P_{Sum}}$ distributions in 2019 and 2021 data, at beam energies of 4.55 GeV and 3.74 GeV respectively, using somewhat different selections. The high $\mathrm{P_{Sum}}$ radiative peak is critical for the minimal A' searches while SIMPs and iDM events require good acceptance for $x = \frac{|p_{e^+}+p_{e^-}|}{E_{\mathrm{beam}}} < 0.8$.

the momentum resolution of the SVT, and can be calibrated against Monte Carlo with elastically scattered full-energy beam electrons (FEE). The FEE momentum distribution compared to the ideal Monte Carlo is shown in Figure 3 for the 2016, 2019, and 2021 datasets, where extensive SVT alignment work is required to bring the resolution as close to the Monte Carlo ideal as possible. Again, the momentum reconstruction with current calibrations for 2019 and 2021 data is similar in quality to the final 2016 calibrations from [11]. The third is the resolution of the e^+e^- vertex position along the beamline as a function of mass, which is used to select against prompt QED backgrounds from the target, and must closely match the Monte Carlo expectation for sensitivity in the displaced searches. This distribution is shown in Figure 4 as a function of mass for all three datasets, where the 2019 and 2021 datasets are expected to have resolution a factor of two better than in the engineering runs because of the SVT upgrade. The reconstruction of vertex position with current calibrations for the 2019 and 2021 data are already closer to ideal Monte Carlo than those from the final 2016 calibrations over the range of masses where sensitivity is expected. While further improvements are anticipated before final reprocessing for 2019 and 2021 data, the calibrations are already similar to, and in some cases closer to ideal Monte Carlo than, the final calibrations for engineering run data shown in [11], enabling analysis of these datasets to proceed.

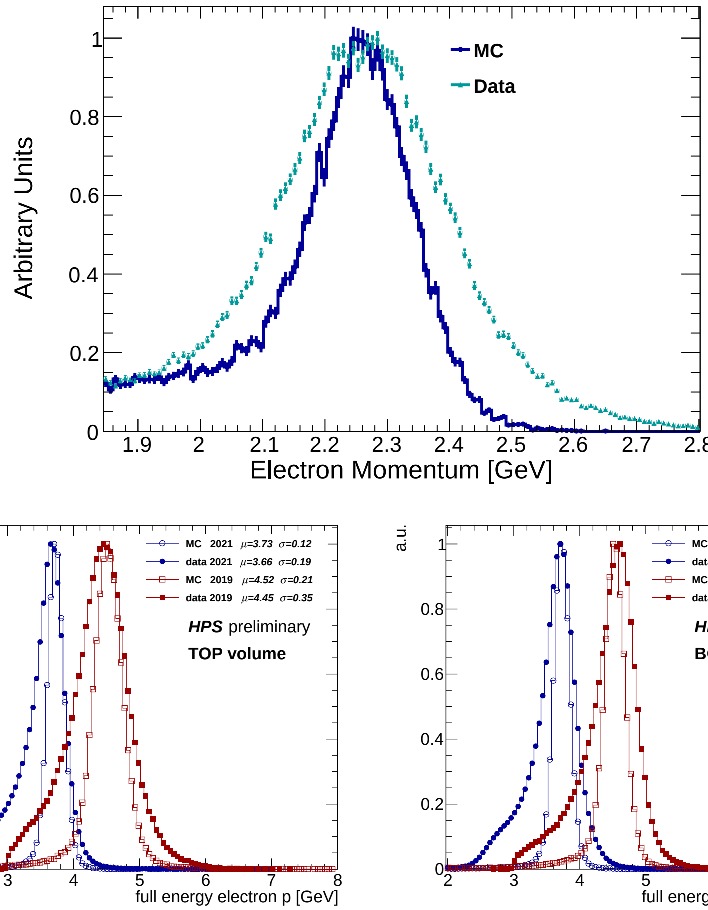

FIG. 3. Top: The momentum distribution of elastically scattered full energy beam electrons (FEE) in 2016 Data and Monte Carlo, where smearing of the Monte Carlo momentum is required for data to match ideal Monte Carlo [11]. Bottom: the same Data/MC comparisons for 2019 and 2021 data using the most recent calibration pass in both the top and bottom halves of the SVT.

3.1. Resonance Search

HPS reported first results of a resonance search with 2015 data [10], and subsequently also with 2016 data [11]. The resonance search is relatively simple in principle, but the extreme statistics of the data create significant challenges. In particular, it is difficult to identify a function that adequately models the background shape over the entire range of e^+e^- mass used in the search. As a result, the typical approach of performing fits in a sliding window has been used: In each mass window, the data is fit with a gaussian for signal plus a generic polynomial background. The complexity of the background shape required to fit the background well at extremely high statistics means that the background model is far from orthogonal to the signal lineshape, eroding the signal sensitivity by a large factor. It is primarily for this reason that the resonance search results, shown in Figure 5, have fallen short of expectations by over an order of magnitude.

To improve the sensitivity of the resonance search, HPS has recently undertaken a concerted effort to identify a single background model for the entire e^+e^- invariant mass distribution. A set of tools has been developed to allow the large-scale automated testing of hundreds of different functions used in similar fits by other experiments and identify promising background models for

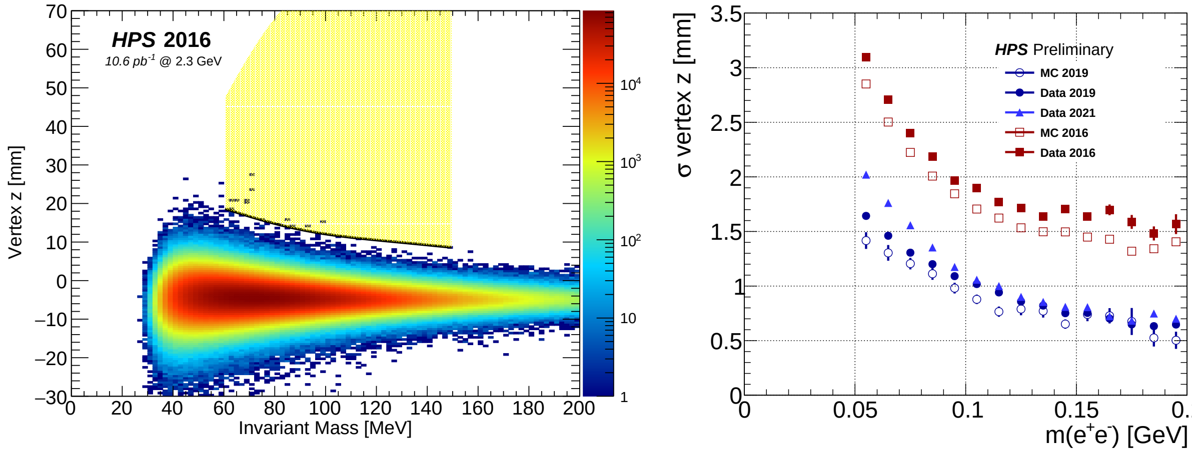

FIG. 4. Left: The mass of the e^+e^- pair vs. the vertex location along the beamline (v_z) after all selections for high-$\mathrm{P}_{\mathrm{Sum}}$ displaced vertex search with 2016 data, with the signal region above a mass-dependent cut in z-vertex position (the "z cut") in yellow [11]. Right: The v_z resolution in Data and Monte Carlo for 2016, 2019, and 2021 using the latest calibration passes, demonstrating the improvement in resolution from the SVT upgrade.

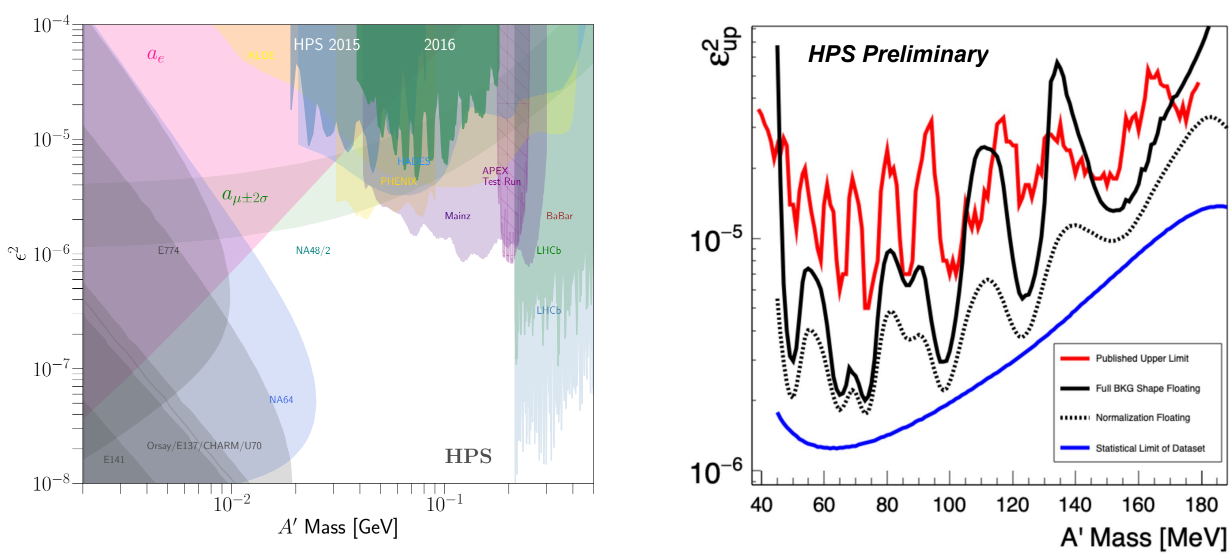

FIG. 5. Left: Results of the resonance searches with engineering run data [10] [11]. Right: The published 2016 result (red) along with results using a global fit shape with all parameters floating (solid black), with only normalization floating (dotted black) and the $\sqrt{N}$ limit on potential signal sensitivity in a sliding two-sigma mass window. Roughly an order-of-magnitude improvement in sensitivity is possible.

the resonance search. Proof of concept tests have been conducted using a candidate function, where Figure 5 shows the potential improvement in sensitivity for the 2016 resonance search in two possible use cases compared to the ultimate statistical limitation of the data. Work is ongoing to develop the set of possible background models and determine how to employ them in an unbiased way for a blind search for 2019 and 2021 data, with the promise of sensitivity that is competitive with collider searches at larger couplings.

3.2. High-P_{Sum} Displaced Vertex Search – minimal A' scenario

HPS has unique and compelling sensitivity in the displaced vertex searches, where the SVT has been designed with this goal in mind. In the case of the high-P_{Sum} search, the sensitivity for the minimal A' model lies in a favored region of parameter space where dark-photon mediated dark matter can explain the full relic abundance, including a range in mass that cannot be reached by other operating or proposed experiments.

Due to multiple scattering effects that dominate the vertex resolution, this search is most difficult at low beam energies, so the 2015 search was far from having new sensitivity, and only reported in a doctoral dissertation [12]. The results of a displaced A' search with HPS was first published with 2016 data, as shown in Figure 6. The sensitivity of this search using the combined 2019 and

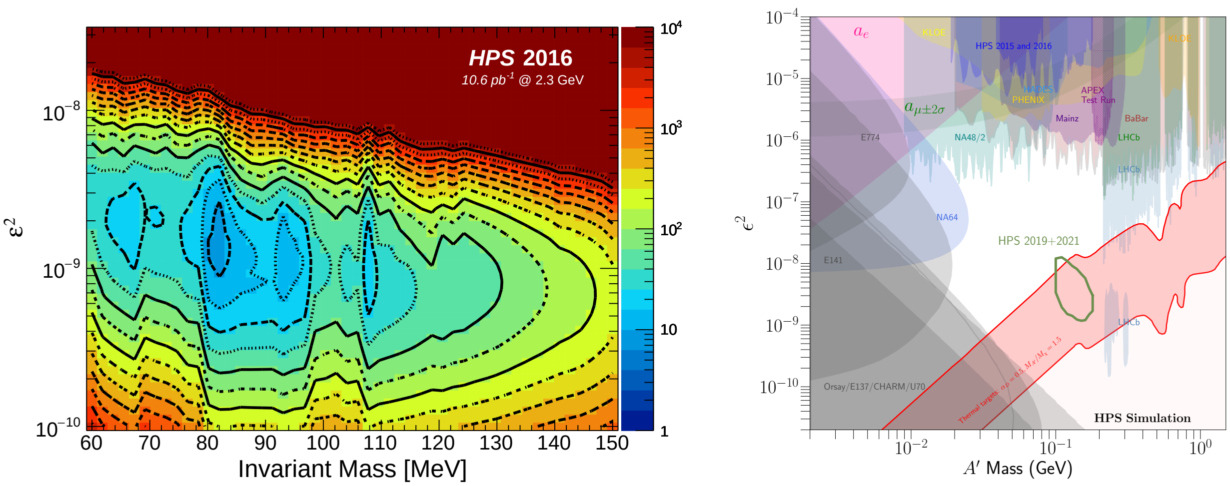

FIG. 6. Left: Results of the high-P_{Sum} displaced search with 2016 data, which achieved sensitivity to A' production at 7.82 times the rate expected for minimal A'. [10] Right: the expected reach of 2019+2021 data assuming similar signal acceptance and background rejection as in the 2016 data.

2021 datasets has been studied, assuming the same analysis techniques and similar backgrounds, and is also shown in Figure 6. Meanwhile, the first low-P_{Sum} search – for SIMPs – has developed new techniques for rejecting backgrounds in displaced searches that are expected to improve the sensitivity of all displaced searches, as will be described in the next section.

3.3. Low-P_{Sum} Displaced Vertex Search - SIMPs and iDM

SIMP and inelastic dark matter models couple to the Standard Model via the same heavy photon mediator but the experimental production rates compatible with thermal production of the observed relic abundance in the early universe can be much larger, so HPS can be sensitive to these models even with smaller datasets. The simplest extension of the minimal A' search is the SIMPs search, which proceeds in the same way as the displaced A' search but selects events with $x < 0.8$ instead of $x > 0.8$.

Because there is a strong likelihood that 2016 data has new sensitivity, and because the systematics for this dataset are already well-understood, the first SIMPs search is being performed on the 2016 engineering run data, which has also been used to develop a number of improvements in event and track reconstruction since the publication of 2016 results. Meanwhile, the SIMPs analysis has also provided a platform for generic improvements to the displaced vertex selections.

In particular, simpler cuts on the impact parameter of the individual electrons and positrons that make up a vertex have proven more powerful than the approach used for the results in Section 3.2, as shown in Figure 7. Analysis of an unblinded 10% sample of 2016 data has been completed and

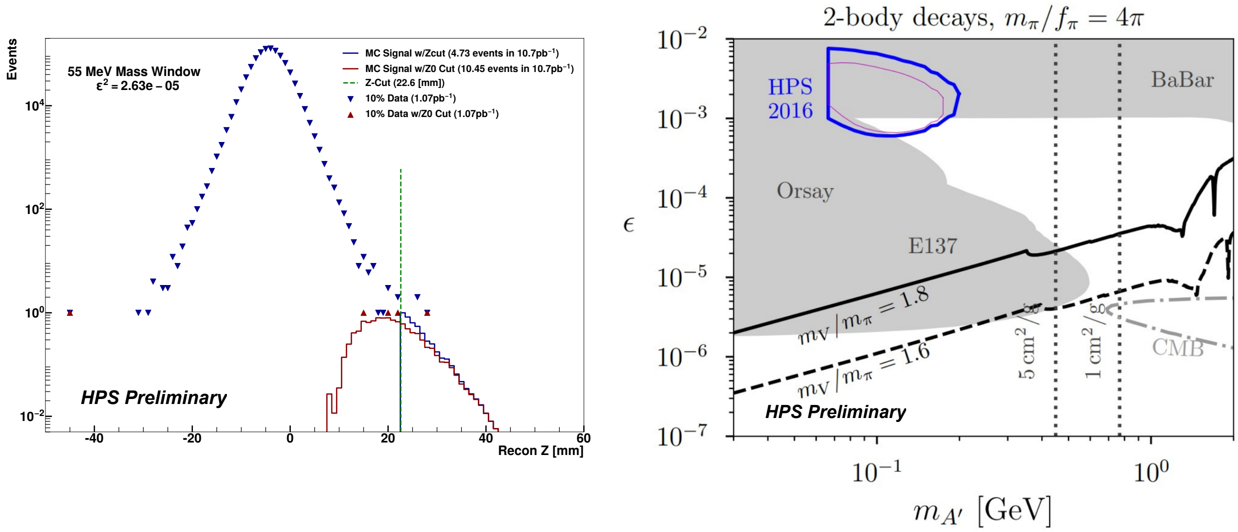

FIG. 7. Left: The signal and background v_z distributions using the selection strategy from [10] that models the prompt background (blue points) and selects events above some v_z (green line – the "z cut"), and a new strategy that nearly eliminates all background (red points) and makes no v_z cut, leading to larger signal efficiency (histograms) for similar background levels. Right, the projected sensitivity for SIMPs using the old(new) displaced vertex selections shown in red(blue), based on analysis of an unblinded 10% sample.

used to project the sensitivity for the full sample for SIMPs, also shown in Figure 7. Unblinding of the full sample and publication of search results are expected alongside with completion of a Ph.D. dissertation later this year. Meanwhile, the improvements developed in the displaced vertex selection will also be applied to the high-P_{Sum} search, and are expected to improve sensitivity to the minimal A' model as well.

Lack of a resonance makes the iDM search significantly more difficult. Also, while production rates can be very large, the kinematics of iDM events are such that the e^+e^- pair are often in the same half (top or bottom) of the detector. Because of this, initial studies have shown that data collected before installation of the scintillation hodoscope, when a trigger for e^+e^- pairs in opposite ECal volumes was used, does not have sensitivity to iDM parameter space. However, these studies suggest that data collected with the positron-only trigger beginning in 2019, are likely to accept significant yields of iDM events, leaving the challenge of discriminating between these events and hard bremsstrahlung that convert in layers of the SVT. Once the other searches on 2019 and 2021 data are completed, the potential for an iDM search with these datasets will be further explored.

4. FUTURE OPERATIONS AND SCIENCE GOALS

Collection of larger datasets at multiple energies is required to achieve the full potential of the HPS experiment. The acceptance of the detector produces sensitivity to A' that spans a range of masses for each beam energy, and with 8-12 weeks at each beam energy, these mass ranges overlap. Accordingly, the ultimate goal of HPS is to collect sufficient data at the available beam energies to provide continuous, overlapping coverage between $\sim 50\,\mathrm{MeV}$ and the di-muon threshold. This region includes parameter space often motivated by sub-GeV thermal dark matter, where a dark photon is the preferred mediator of DM-SM interactions responsible for setting the observed dark matter abundance through freeze-out: the so-called "thermal targets."

With 105 PAC days remaining, studies show that HPS has the largest overall region of sensitivity with 40 days of operation with a one-pass ($\approx 2\,\text{GeV}$) beam and the remainder with a two-pass ($\approx 4\,\text{GeV}$) beam. The ultimate sensitivity of HPS for this run plan in the key benchmark of the displaced minimal A' search is shown in Figure 8. HPS has requested beam time in the schedule

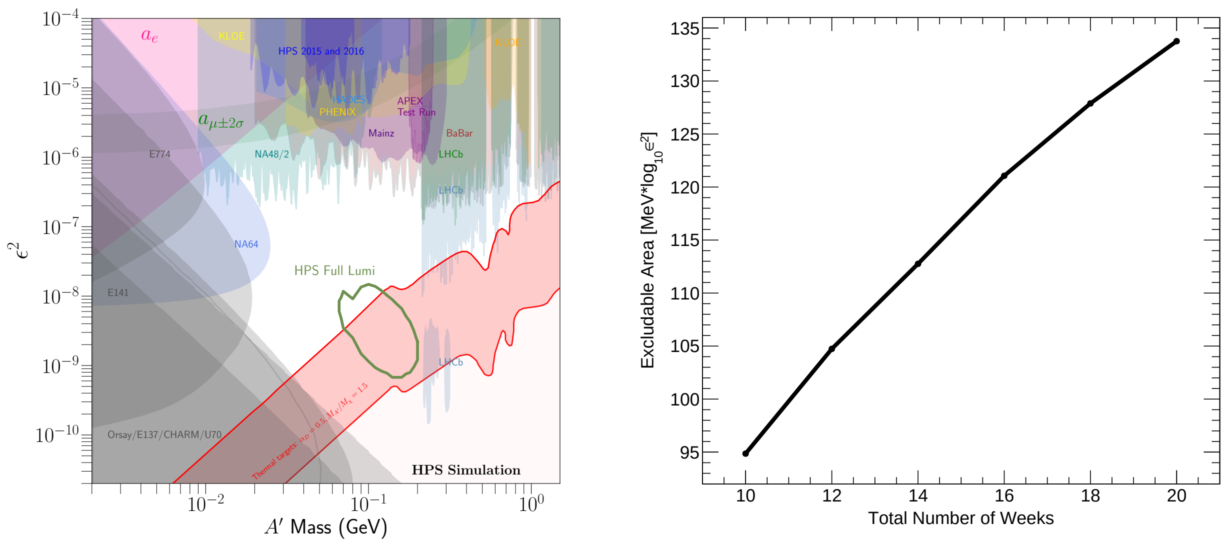

FIG. 8. Left: The projected sensitivity of HPS in the displaced minimal-A' search after completing the run plan presented in the text. Right: The area of sensitivity for this search as a function of the total number of weeks of two-pass running, showing that HPS will not reach a sensitivity plateau in the most favored area of parameter space before consuming the approved beam time, 12.8 weeks total at 50% efficiency.

being planned for late 2025 or 2026 and is beginning to prepare the detector for operations. Because the sensitivity and complementarity of HPS with other experiments is best in the region covered with two-pass operation – just below the di-muon threshold – this run is again being planned with a two-pass beam. Once we have final results from 2019/2021 analysis, we will assess whether to use the remainder of HPS beam time on one-pass running as discussed above or whether there is a stronger case to have more data at $\approx 4\,\text{GeV}$, where studies have shown that the region of sensitivity for the experiment with two-pass beam continues to grow almost linearly even beyond the full beam time allocated to the experiment, as shown in Figure 8.

---

[1] M. Battaglieri *et al.* [arXiv:1707.04591 [hep-ph]].

[2] B. Holdom, Phys. Lett. B **166**, 196-198 (1986) doi:10.1016/0370-2693(86)91377-8.

[3] A. Grillo *et al.* [HPS Collaboration], `https://www.jlab.org/exp_prog/PACpage/PAC37/proposals/Proposals/New%20Proposals/PR-11-006.pdf`

[4] M. Battaglieri *et al.*, [HPS Collaboration], Nucl. Instrum. Meth. A **777**, 91-101 (2015) [arXiv:1406.6115 [physics.ins-det]]

[5] P. Hansson Adrian *et al.*, [HPS Collaboration], `https://www.jlab.org/exp_prog/proposals/12/C12-11-006.pdf`

[6] N. Baltzell *et al.* [HPS], Nucl. Instrum. Meth. A **859**, 69-75 (2017) [arXiv:1612.07821 [physics.ins-det]].

[7] I. Balossino *et al.* [HPS], Nucl. Instrum. Meth. A **854**, 89-99 (2017) [arXiv:1610.04319 [physics.ins-det]].

[8] A. Berlin *et al.*, Phys. Rev. D **97**, 055033 (2018)
[9] P. Harris, P.Schuster, J. Zupan, [arXiv:2207.08990[hep-ph]]
[10] P. Adrian *et al.* [HPS], Phys. Rev. D **98**, no.9, 091101 (2018) [arXiv:1807.11530 [hep-ex]].
[11] P. Adrian *et al.* [HPS], Phys Rev. D **108**, no.1, 012015 (2023) [arXiv:2212.10629 [hep-ex]]
[12] S. Uemura, Stanford University (2016), https://purl.stanford.edu/hs558pd7550